

LKB1/STRAD Promotes Axon Initiation During Neuronal Polarization

Maya Shelly,¹ Laura Cancedda,¹ Sarah Heilshorn,^{1,2} Germán Sumbre,¹ and Mu-ming Poo^{1,*}

¹Division of Neurobiology, Department of Molecular and Cell Biology, Helen Wills Neuroscience Institute, University of California, Berkeley, CA 94720

²Present address: Department of Materials Science and Engineering, Geballe Laboratory for Advanced Materials, Stanford University, Stanford, CA 94305, USA.

*Correspondence: mpoo@uclink.berkeley.edu

DOI 10.1016/j.cell.2007.04.012

SUMMARY

Axon/dendrite differentiation is a critical step in neuronal development. In cultured hippocampal neurons, the accumulation of LKB1 and STRAD, two interacting proteins critical for establishing epithelial polarity, in an undifferentiated neurite correlates with its subsequent axon differentiation. Downregulation of either LKB1 or STRAD by siRNAs prevented axon differentiation, and overexpression of these proteins led to multiple axon formation. Furthermore, interaction of STRAD with LKB1 promoted LKB1 phosphorylation at a PKA site S431 and elevated the LKB1 level, and overexpressing LKB1 with a serine-to-alanine mutation at S431 (LKB1^{S431A}) prevented axon differentiation. In developing cortical neurons in vivo, downregulation of LKB1 or overexpression of LKB1^{S431A} also abolished axon formation. Finally, local exposure of the undifferentiated neurite to brain-derived neurotrophic factor or dibutyl-AMP promoted axon differentiation in a manner that depended on PKA-dependent LKB1 phosphorylation. Thus local LKB1/STRAD accumulation and PKA-dependent LKB1 phosphorylation represents an early signal for axon initiation.

INTRODUCTION

Neuronal polarization may involve an initial specification of axon/dendrite identity of the undifferentiated neurites, followed by selective trafficking and segregation of components into the axon and dendrites (Craig and Banker, 1994; Arimura and Kaibuchi, 2007). The asymmetry of cytoplasmic components following the last mitotic division (de Anda et al., 2005) or extracellular polarizing signals (Adler et al., 2006) may cause the initial asymmetry in the distribution of a key component that specifies the axon. In the absence of intrinsic or extrinsic signals, stochastic accumulation of such a component in one neurite,

if amplified by local positive feedback, may result in a stable signal for axon initiation. Since the first morphological sign of axon differentiation is an accelerated neurite growth, the initial event may specify the axon fate simply by accelerating the neurite growth.

Dissociated hippocampal neurons in culture have been widely used for studying neuronal polarization (Dotti et al., 1988). Using this system, many signaling molecules were found to be essential for neuronal polarization, including an axon-specific microtubule-associated protein CRMP-2 (Inagaki et al., 2001), the mammalian partitioning-defective (PAR) proteins PAR-3 and PAR-6 (Shi et al., 2003), the small GTPases Rap1B and Cdc42 (Schwamborn and Puschel, 2004), GSK-3 β and its upstream regulators such as PI3K and PTEN (Shi et al., 2003; Jiang et al., 2005; Yoshimura et al., 2005), the plasmalemma ganglioside sialidase (Da Silva et al., 2005), PAR-1 related SAD kinases (Kishi et al., 2005), the plus-end motor proteins KIF3A (Nishimura et al., 2004) and KIF5C (Jacobson et al., 2006), the MARK2 (Chen et al., 2006), the insulin-like growth factor-1 (Sosa et al., 2006), and a neuron-specific protein shootin1 (Toriyama et al., 2006). Perturbing the activity of these molecules often abolishes axon differentiation or causes multiple axon formation.

In *C. elegans*, the six PAR genes (*par-1* through *par-6*) function as master regulators of cell polarity, and the PAR-3/PAR-6/aPKC complex is crucial for the development of epithelial polarity in *Drosophila* and mammals (Wodarz, 2002). The involvement of PAR-3/PAR-6 in neuron polarization indicates that mechanisms governing polarity formation are conserved across cell types and suggests that other determinants of epithelial polarity may also play a role in neuronal polarization. In the present study, we focused on the LKB1/STRAD/MO25 complex, an early determinant of epithelial polarization (Baas et al., 2003, 2004; Boudeau et al., 2003; Alessi et al., 2006). The serine/threonine kinase LKB1 is a homolog of PAR-4. Upon complex formation with the STE20-related pseudokinase (STRAD) and a ubiquitously protein MO25, LKB1 is activated, stabilized, and translocated from the nucleus to the cytoplasm (Baas et al., 2003). In single isolated epithelial cells, LKB1 activation induced by the expression of STRAD leads to cell-autonomous execution of a complete polarization program (Baas et al., 2004).

The phosphorylation of LKB1 on a C-terminal serine, S431, by agonist-activated, cAMP-dependent protein kinase (PKA) is important for its function in cell-cycle regulation (Sapkota et al., 2001) and polarity formation in *Drosophila* (Martin and St Johnston, 2003). In this work, we found evidence in support of the notion that accumulation of LKB1/STRAD complex and PKA-dependent phosphorylation of LKB1 in an undifferentiated neurite represent an early signal for axon initiation.

RESULTS

LKB1 Localization in Axon and Undifferentiated Neurites

Dissociated embryonic hippocampal neurons in culture initially extended several undifferentiated neurites. Within 24 hr after cell plating one of the neurites exhibited accelerated growth and showed axon-specific markers (e.g., Tau-1 and smi-312; Sternberger et al., 1982; Figure S1) but not the dendrite-specific marker MAP2. Immunostaining of LKB1 and Tuj-1, a neuron-specific class III β -tubulin, showed higher levels of LKB1 in axons than those in dendrites (Figures S2A and S2B). The distribution of LKB1 in polarized neurons was quantified by measuring the average intensity of LKB1 immunofluorescence in each neurite, normalized by that of the soma (Figure S2B). Distinct higher levels of LKB1 were found in axons (with high smi-312 staining) than that in dendrites (with high MAP2 staining). Although most cells develop a single axon (SA) and multiple dendrites, a small population of cells exhibited either multiple axons (MA) or no axon (NA). The total LKB1 staining of the cell, normalized by total Tuj-1 staining, correlated well with axon differentiation; it was lowest in NA cells and highest in MA cells (Figure S2C). Thus LKB1 is localized specifically in differentiated axon, and its expression level correlates with the extent of axon formation. Interestingly, in unpolarized neurons 6–12 hr after plating, we found many neurons exhibited high LKB1 immunostaining in one neurite (Figure 1A). By defining LKB1 accumulation as LKB1 immunostaining intensity (normalized by Tuj-1 staining) higher by more than 0.5 SD above the mean intensity of all neurites, we found that 40% (30/75) of the cells showed LKB1 accumulation in a single neurite, 48% showed LKB1 accumulation in more than one neurite, and the rest showed no accumulation in all neurites. When the average LKB1 staining of each neurite was plotted in an order of intensity for up to seven neurites for all cells (Figure 1Ba), the LKB1 level in the most enriched neurite was 2–4 times that of other neurites of the same neuron, whereas its length was not significantly different (Figure 1Bb). Thus, distinct LKB1 localization in one neurite often occurred prior to axon differentiation.

Coaccumulation of LKB1 and STRAD in Undifferentiated Neurites

In epithelial polarization, STRAD is an essential cofactor for the LKB1 function (Baas et al., 2004). The RT-PCR

assay showed that mRNAs of LKB1 and STRAD were expressed in E18 rat hippocampus and cortex (Figure S3A) and that the expression persisted in P7 and P14 rats. Coimmunoprecipitation studies using HEK-293T cells transfected with vectors containing rat STRAD and LKB1 cDNAs confirmed the interaction between STRAD and LKB1 (Figure S3B). Moreover, GFP immunoblots of total HEK293T cell lysates showed that LKB1 and STRAD caused mutual stabilization upon coexpression, with their protein levels increased by 5- and 2-fold, respectively (Figure 1C). We further examined whether there is a preferential coaccumulation of LKB1 and STRAD in a single neurite prior to neuronal polarization. Since no suitable antibody for STRAD immunostaining was available, we transfected cultured hippocampal neurons with GFP-STRAD at 4 hr after cell plating and examined the cells at 16 hr (Figures 1D and 1E). The level of total GFP-STRAD expression varied greatly among transfected cells (Figure S3C). While many cells exhibited GFP-STRAD accumulation in multiple neurites at 16 hr, one-third (29/85) showed distinct GFP-STRAD accumulation in a single neurite. Measurements of the total GFP intensity of the neuron showed that GFP-STRAD accumulation in multiple neurites indeed correlated with higher GFP-STRAD expression (Figure S3C). Interestingly, half of the cells with GFP-STRAD accumulation in a single neurite (15/29) also exhibited accumulation of LKB1 immunostaining in the same neurite (Figure 1E). This coaccumulation is highly significant, as shown by bootstrap analysis of the probability of coaccumulation by chance ($p < 2.5 \times 10^{-13}$; see Supplemental Experimental Procedures). Measurements of the average GFP-STRAD and LKB1 immunostaining (normalized by Tuj-1 staining) of all neurites of these 29 cells also indicated a preferential enrichment of these two proteins in the same neurite (Figures 1Da and 1Db), which had a length similar to other neurites of the same cell (Figure 1Dc). Thus, under low-level GFP-STRAD expression, LKB1 and GFP-STRAD often coaccumulate in a single neurite of the unpolarized neuron.

GFP-STRAD Accumulation Predicts Axon Fate

We further followed the fate of neurites exhibiting GFP-STRAD accumulation in live cells over a 2 day period. GFP-LKB1 was not used because the GFP-LKB1 expression resulted in a high frequency of multiple axon formation (Figures 3E and S4). In many GFP-STRAD-transfected cells, neurites with distinct GFP-STRAD accumulation at 16 hr mostly became axons by 48 hr, when accumulation occurred in either a single neurite (Figure 2A) or multiple neurites (Figure 2B), and GFP-STRAD accumulation persisted after axon differentiation (Figure 1F). Further analysis was performed on the entire population of GFP-STRAD-transfected neurons that were imaged at both 16 and 48 hr ($n = 73$). Neurons were divided into two groups according to the GFP-STRAD distribution at 16 hr: accumulation in a single neurite (Group I, $n = 30$) or in multiple neurites (Group II, $n = 43$). For all Group I neurons, single axon (SA) formation was observed at 48 hr,

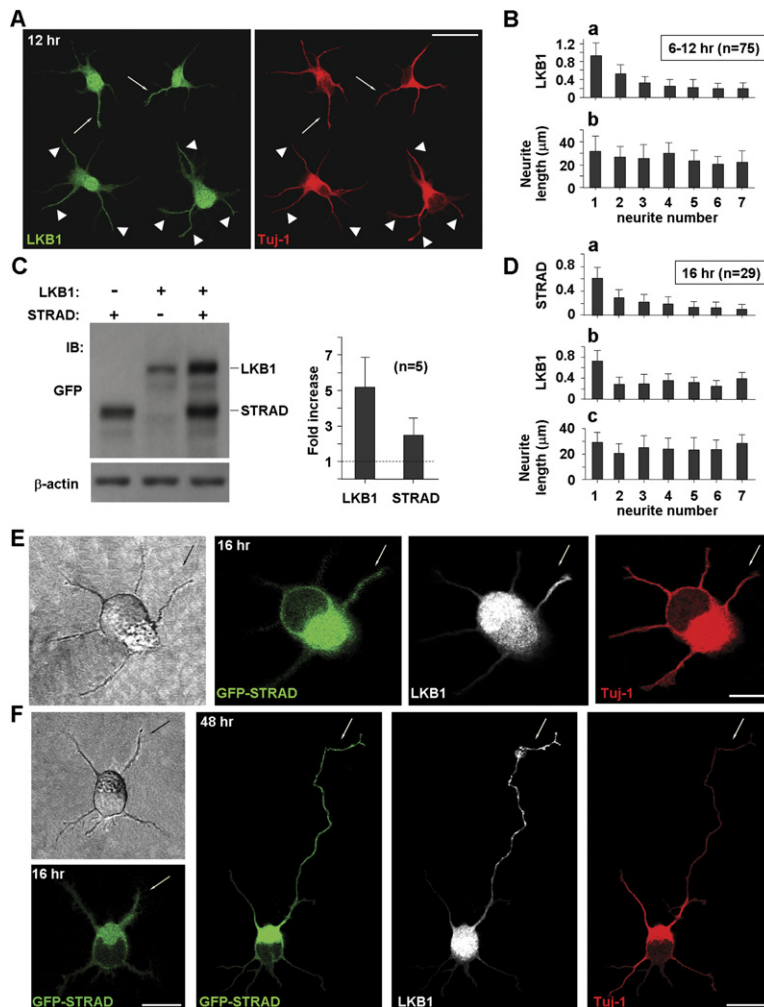


Figure 1. Accumulation of LKB1 and STRAD in Undifferentiated Neurites and Axons

(A) Hippocampal neurons in 12 hr cultures, coimmunostained for LKB1 and neuron-specific marker Tuj-1, showing LKB1 accumulation in either one neurite (arrows) or multiple neurites (arrowheads). Scale is 30 μm.

(B) LKB1 accumulation in undifferentiated neurites (in 6–12 hr cultures). (a) Mean LKB1 immunofluorescence intensity for each neurite (normalized to that of Tuj-1) plotted in the order of intensity for the first seven neurites of each cell, averaged over all cells (\pm SD, $n = 75$). (b) Average neurite length, corresponding to that in (a).

(C) Left: Immunoblots of total cell lysates of HEK293T cells transfected with rat GFP-STRAD and GFP-LKB1, either alone or together. Right: Average fold increases (\pm SD, $n = 5$) in the GFP-STRAD and GFP-LKB1 level upon coexpression as compared to their level when transfected alone (each normalized to β -actin).

(D) LKB1 and GFP-STRAD colocalization in hippocampal neurons in 16 hr cultures. Neurons were transfected with GFP-STRAD 4 hr after plating and immunostained for LKB1 and Tuj-1 at 16 hr. (a) Mean fluorescence intensity of GFP-STRAD for each neurite (normalized to that of Tuj-1) for 29 cells (\pm SD, same data set as in Figure S3C), arranged in the order of the GFP-STRAD intensity for the first seven neurites of each cell and showing preferential accumulation in a single neurite. (b) The mean LKB1 level in each neurite corresponding to those arranged in (a). (c) Average length of the neurites shown in (a) and (b).

(E) A GFP-STRAD-transfected neuron, stained for LKB1 and Tuj-1 at 16 hr, showing LKB1 and GFP-STRAD colocalization in a single neurite (arrow). Scale is 10 μm.

(F) GFP-STRAD expression in a neuron at 16 and 48 hr, costained for LKB1 and Tuj-1 at 48 hr. Scales are 10 μm (16 hr) and 25 μm (48 hr).

and the neurite with the highest level of GFP-STRAD (Figure 2Ca) was not significantly different in length from other neurites of the same cell (Figure 2Cb). Furthermore, for a majority of Group I cells (18/30) the neurite that showed GFP-STRAD accumulation became the axon (Figure 2Cc). Moreover, by 48 hr, GFP-STRAD fluorescence of most of these 30 cells was high in axons but low in dendrites (Figure S3D). For Group II neurons ($n = 43$) that showed GFP-STRAD accumulation in multiple neurites at 16 hr, we found 23 SA, 16 MA, and 4 NA cells at 48 hr. For SA cells, GFP-STRAD distribution was relatively uniform in all neurites at 16 hr (Figure 2Cd), and the axon emerged randomly among all neurites at 48 hr (Figure 2Cf). For MA cells, there was a more steep gradient of GFP-STRAD intensity among all neurites at 16 hr (Figure 2Cg), and axons emerged with a higher probability from neurites that had higher GFP-STRAD level at 16 hr (Figure 2Ci). Bootstrap analysis for all SA cells (including both Groups I and II, $n = 53$) showed that the probability for 30 axons to emerge from the GFP-STRAD-accumulat-

ing neurites among all neurites of these 53 cells (18/30 in Group I and 12/23 in Group II) by chance is extremely low ($p = 5 \times 10^{-8}$, Supplemental Experimental Procedures). Thus, the neurite exhibiting GFP-STRAD accumulation is most likely to become the axon. Finally, the total GFP-STRAD fluorescence of each of the 73 cells at 16 hr was significantly higher for Group II SA or MA cells than for Group I SA cells (Figure 2D), consistent with the idea that GFP-STRAD overexpression promotes multiple axon formation.

Effects of Downregulating or Overexpressing LKB1/STRAD

To more directly address the role of LKB1 and STRAD in axon differentiation, we prepared small interference RNAs (siRNAs) targeted to either rat LKB1 or STRAD mRNAs (two sequences for each) and conjugated them with fluorescein; their efficiency in downregulating the expression of GFP-LKB1 and GFP-STRAD was confirmed in 293T cells (Figures 3A and 3B). Furthermore, both LKB1

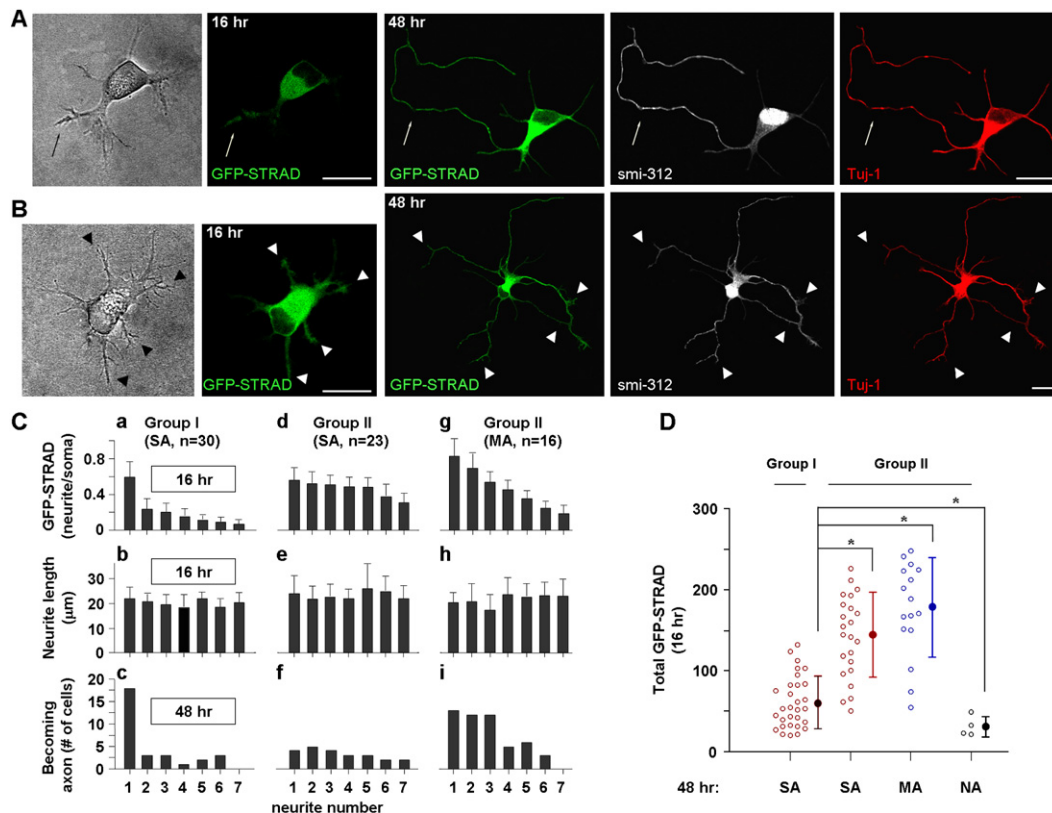


Figure 2. GFP-STRAD Accumulation in Undifferentiated Neurite Predicts Axon Fate

(A and B) Two GFP-STRAD-transfected neurons, imaged at 16 and 48 hr and costained for Tuj-1 and smi-312 at 48 hr, showing the formation of either a single axon (A, arrow) or multiple axons (B, arrowheads). Scale is 20 μ m.

(C) GFP-STRAD distribution in all undifferentiated neurites at 16 hr for 73 neurons and the correlation between GFP-STRAD accumulation at 16 hr and axon differentiation at 48 hr. Group I ($n = 30$): single neurite accumulation; Group II ($n = 43$): accumulation in more than one neurite. Group II neurons were further divided according to polarization phenotype at 48 hr: SA, single axon ($n = 23$); MA, multiple axons ($n = 16$); and NA, no axon ($n = 4$). Error bars indicate \pm SD. Histograms depict the average GFP-STRAD intensity for each neurite at 16 hr (normalized to that of the soma) plotted in the order of intensity for the first seven neurites of each cell (a, d, and g), the average length of these neurites (b, e, and h), and the number of cells in which the corresponding neurites shown in (a), (d), and (g) became axons at 48 hr (c, f, and i).

(D) Total GFP-STRAD fluorescence intensity (including all processes and soma) at 16 hr for all Group I and II cells ($n = 73$) shown in (C), presented according to polarization phenotypes at 48 hr. Each point depicts one cell, and points with error bars depict average \pm SD. A significant difference was found among the four groups (nonparametric ANOVA; Friedman's test, $p < 0.01$), and that between two groups is marked by the asterisk ($p < 0.01$, Kolmogorov-Smirnov test).

siRNAs downregulated the endogenous LKB1 expression in cultured hippocampal neurons (Figures 3Ca and 3Cb), with siRNA-1 exhibiting a higher efficiency, while the control LKB1 siRNA (harboring two point mutations in the siRNA sequence) had no effect (Figures 3Ca and 3Cb). Cells transfected with LKB1-siRNA-1 exhibited lower levels of LKB1 (Figure 3Da) and showed no axon differentiation (Figure 3Db) 4 days after transfection, whereas those expressing control LKB1-siRNA (Figure 3Dd) and untransfected cells (Figures 3Da–3Dc) showed normal axon differentiation. Interestingly, MAP2 staining showed no dendrite differentiation in these nonpolarized cells, which had grown extensive neurites (Figure 3Dc). Similar reduction in SA cells and an increase in NA cells were observed following transfection with either LKB1 or STRAD siRNAs, but the total neurite length of each neuron was

not affected (Figure 3E). Thus, downregulation of LKB1 or STRAD inhibits axon differentiation without affecting the overall neurite growth. Inefficient downregulation of LKB1 may account for the normal polarization of some LKB1 siRNA-1-transfected neurons since when the total LKB1 level of transfected cells was randomly sampled we found that NA cells had a significantly lower LKB1 level than SA cells (Figure 3F). Finally, overexpression of LKB1 resulted in a high percentage of MA cells when examined 4 days later (Figures 3E and S4), similar to that caused by GFP-STRAD overexpression (Figures 2B and 2D).

Cyclic AMP- and BDNF-Induced LKB1 Phosphorylation and Stabilization

In epithelial cells, STRAD/LKB1 complex formation leads to LKB1 phosphorylation, which is necessary for LKB1

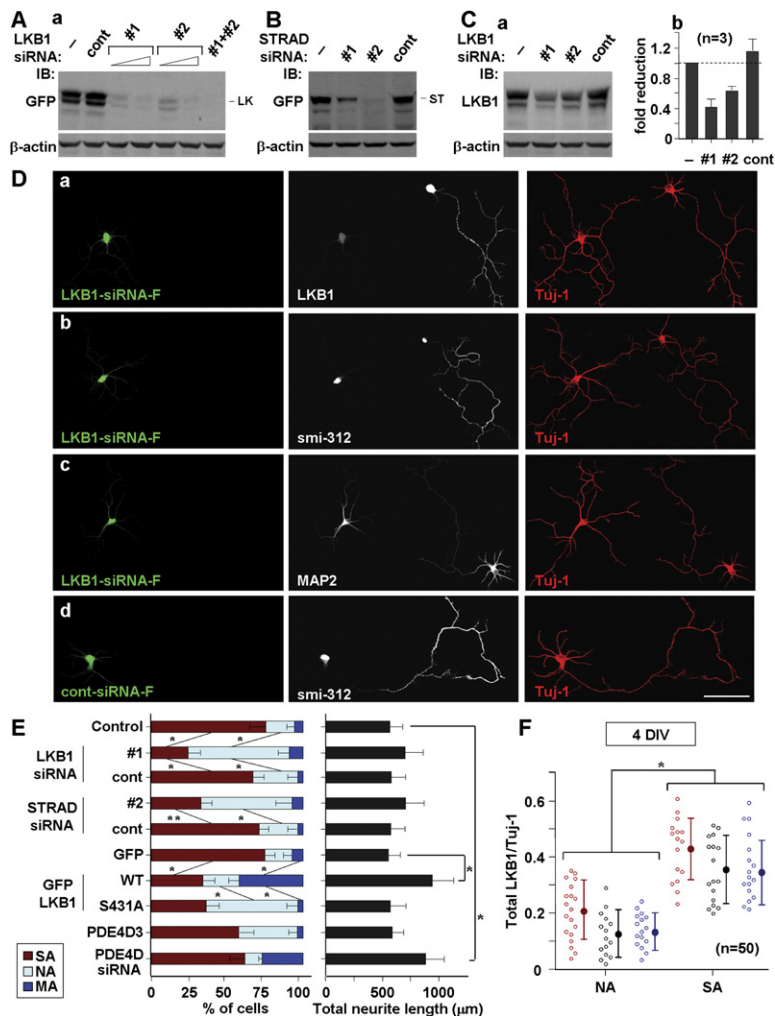


Figure 3. Effects of LKB1/STRAD Down-regulation and LKB1 Overexpression

(A and B) Downregulation of LKB1 and STRAD in HEK293T cells by siRNA. Two fluorescein-tagged siRNA duplexes (sequence #1 and #2) targeting rat LKB1 (A) or STRAD (B) and their respective control siRNAs ("cont") were each transfected in HEK293T cells together with GFP-LKB1 (A) or GFP-STRAD (B). (A: #1 and #2 alone, 30 and 100 nM; control or #1 + #2, 30 nM each. B: 30 nM each). Total cell lysates were prepared for immunoblotting 48 hr after transfection. "-" indicates lysates of untransfected cells.

(C) Downregulation of LKB1 in hippocampal neurons by siRNA. Transfection of LKB1 siRNAs (30 nM) and immunoblotting were performed as in (A). LKB1 level is quantified as the fold reduction (\pm SD, $n = 3$) relative to untransfected cells (marked "-") normalized to β -actin.

(D) Neurons in 4 DIV cultures transfected with fluorescein-tagged LKB1-siRNA-1 or its control siRNA. Cells were costained with Tuj-1 together with LKB1 (a), smi-312 (b and d), or MAP2 (c). One untransfected cell is shown in (a)-(c). Scale is 50 μ m.

(E) Summary of effects of downregulating LKB1, STRAD, and PDE4D and of overexpressing LKB1 and PDE4D3, as shown by three cell phenotypes (SA, NA, and MA) observed at 4 DIV. Data depict average percentage (\pm SD) from five different cultures (\sim 40-50 cells each) for each condition. Right: average total neurite length (\pm SD) of each cell for all cells is shown on the left. "Control" indicates untransfected. "Cont" indicates control siRNA. Significant differences between the two groups connected by the line are marked ("*" indicates $p < 0.01$; "****" indicates $p < 0.05$; Kolmogorov-Smirnov test).

(F) LKB1 level in NA and SA neurons transfected with LKB1 siRNA at 4 DIV. Total LKB1 immunofluorescence intensity of each cell (normalized by that of Tuj-1) for 50 random sampled cells from three cultures (coded by color) grouped by polarization phenotypes. Data points with error bars depict the average \pm SD. The difference between NA and SA groups of the same culture or all cultures together was significant ($p < 0.01$, Kolmogorov-Smirnov test).

function. We thus inquired whether cAMP-dependent phosphorylation of LKB1 is involved in neuronal polarization. We first examined the regulation of LKB1 by forskolin, which elevates endogenous cAMP synthesis, in 293T cells transfected with GFP-LKB1. Because STRAD/LKB1 interaction is known to increase the LKB1 level and LKB1 phosphorylation at several sites (Figure 1C; Baas et al., 2003), we also cotransfected the cells with GFP-STRAD as a positive control. Immunoblotting using phosphorylated site-specific antibodies for LKB1 indicated that bath application of forskolin caused an increased LKB1 phosphorylation at the PKA site S431 but not at a nonPKA site T366 (Figure 4A). Similar phosphorylation was also induced by BDNF in cells cotransfected with GFP-LKB1 and TrkB. This increased LKB1 phosphorylation was markedly reduced by the specific PKA inhibitor KT5720 (200 nM) or the competitive cAMP analog Rp-cAMPS. Importantly, the increased LKB1 phosphorylation correlated with an

elevated level of the total LKB1 protein, suggesting that S431 phosphorylation stabilizes LKB1 protein level, possibly through increased heterotrimeric LKB1/STRAD/MO25 complex formation (see below). Exposure to forskolin or BDNF had no effect on LKB1 phosphorylation in 293T cells transfected with a mutant form of LKB1 that has either a deletion of the last ten amino acids at the C terminus that includes S431 (Δ c-ter-LKB1) or a serine-to-alanine point mutation at 431 (LKB1^{S431A}). Furthermore, cotransfection of GFP-STRAD and GFP-LKB1 led to an increased LKB1 phosphorylation at both S431 and T366, and the increased T366 phosphorylation was not affected by transfection with the above mutant LKB1 (Figure 4Aa). Thus, forskolin and BDNF can trigger specific PKA-dependent LKB1 phosphorylation at S431 and increase the LKB1 level, and these effects can also be induced by the coexpression of STRAD. Similar results were also obtained in cultured hippocampal neurons (Figure 4B), although the

GST-STRAD was increased in the presence of GST-MO25 (Figure 4D), indicating that MO25 enhanced LKB1/STRAD interaction. Thus, PKA-dependent phosphorylation of LKB1 is accompanied by the stabilization of the MO25, which in turn serves as a scaffold to promote STRAD/LKB1 interaction, leading to further increase in local LKB1 phosphorylation and accumulation. This positive feedback for the amplification of localized LKB1 phosphorylation in the undifferentiated neurite may be essential for axon initiation (see Figure 7E).

Localization and Function of pLKB1-S431 during Axon Differentiation

Further immunostaining studies showed that the phosphorylated form of LKB1 (pLKB1-S431) was concentrated in the axon but was excluded from the dendrites of polarized neurons in 60 hr cultures (Figure S5A). In 6–12 hr cultures prior to axon differentiation, pLKB1-S431 frequently showed accumulation in one neurite (Figure S5B). Similar analysis as that described for LKB1 (Figure 1B) showed that pLKB1-S431 often preferentially accumulated in a single neurite prior to axon differentiation. Furthermore, transfection of hippocampal neurons with GFP-tagged LKB1^{S431A} markedly reduced axon differentiation (Figures 3E and S5C), suggesting that phosphorylation of LKB1 at S431 promotes axon differentiation.

Downregulating LKB1 or Overexpressing LKB1^{S431A} Abolishes Axon Formation In Vivo

To further explore the importance of LKB1 and its PKA-dependent phosphorylation in axon differentiation in vivo, we used the in utero electroporation method (Saito and Nakatsuji, 2001) to downregulate LKB1 expression or to interfere with LKB1 function. Two LKB1-siRNA and control-LKB1-siRNA sequences (Figure 3) were cloned into the pRNAT-U6.3 expression vector that also drives the expression of EGFP. The LKB1 and LKB1^{S431A} were cloned in the pCAG-IRES-EGFP vector. Since EGFP expression from different constructs may vary, the LKB1 constructs were coelectroporated with a separate vector pCAG-IRES-tdTomato expressing a red fluorescence protein tdTomato. The constructs were injected into the lateral ventricle of E18 rat embryos and electroporated into a subpopulation of neural progenitor cells. After allowing in vivo development, brain slices were obtained from rat pups at P7, and images of cortical neurons that were derived from transfected progenitor cells were acquired by using tdTomato fluorescence, which was found to colocalize with EGFP in ~95% of transfected cells. At P7, cortical axons were well developed, as shown by intense smi-312 immunostaining near the subventricular zone (SVZ) that colocalized with pLKB1-S431 but not MAP2 immunostaining (Figure 5A). In all experimental conditions, tdTomato-positive neurons were mostly located in layer II/III by P7 (Figure 5B), the normal destination for cortical pyramidal cells derived from progenitor cells transfected at E18 (Saito and Nakatsuji, 2001). In comparison to neurons transfected with empty vectors or control-siRNA, we found

that neurons transfected with LKB1-siRNA or LKB1^{S431A} showed a striking absence of axons, as shown by the absence of fluorescently labeled, radially oriented axons throughout cortical layers and of horizontally oriented axons near SVZ (Figures 5B and 5C). Typical transfected neurons and reconstructed cells in layer II/III are shown in Figures 5D and 5E. The same result was found in five embryos each for LKB1-siRNA and LKB1^{S431A} transfection. Thus, either downregulation of LKB1 or overexpression of LKB1^{S431A}, which presumably exerts dominant-negative suppression of normal function of pLKB1-S431, resulted in defects in axon formation in cortical neurons.

The effect of LKB1^{S431A} on axonal formation was not due to overexpression of LKB1 protein itself but to the specific mutation on LKB1 since overexpressing wild-type LKB1 resulted in prevalent axons in the cortical plate and SVZ (Figures 5B and 5C). Interestingly, in latter cortices transfected neurons exhibited abnormal axonal branching and a higher number of long processes descending toward the white matter (Figures 5D and 5E). Coimmunostaining of these abnormal processes with axon-specific markers was not successful due to dense axon staining from nontransfected cells. Moreover, transfected cells in the intermediate zone and SVZ showed complex morphology and apparently retarded migration (Figure 5B, arrowheads), possibly due to multiple axon formation during radial migration. In addition, elevating endogenous cAMP in these cortical neurons by downregulating PDE4 with PDE4D-siRNA resulted in similar abnormal axon differentiation as that found for LKB1 overexpression (Figure S6), further supporting the importance of cAMP signaling in axon differentiation. In embryos cotransfected with LKB1 and STRAD, transfected cells failed to undergo radial migration and mostly accumulated in SVZ (data not shown). Taken together, these in vivo findings indicate that LKB1 is required for axon formation in vivo and that specific PKA-dependent phosphorylation of LKB1 is essential.

Localized BDNF or dB-cAMP Exposure Promotes Axon Differentiation

Given that BDNF induces LKB1 phosphorylation at S431, we further inquire whether localized application of BDNF or dB-cAMP, a membrane-permeable cAMP analog, can provide an instructive signal for axon differentiation. Hippocampal neurons were plated on culture substrates on which BDNF or dB-cAMP was coated in defined stripes (see Supplemental Experimental Procedures), and the fate of neurites in contact with striped and nonstriped regions (both 50 μ m in width) was analyzed. First, we found that a great majority of axon tips of polarized neurons in 60 hr cultures were located on the BDNF, dB-cAMP, or rolipram stripes (Figures 6A and 6Ba), as shown by the high preference index (PI, defined as [(% on stripe)–(% off stripe)]/100%), whereas no preference was found for BSA or NGF stripes. This preferential axon-tip location on stripes may result from chemotropic turning of differentiated axons toward higher concentrations of dB-cAMP or

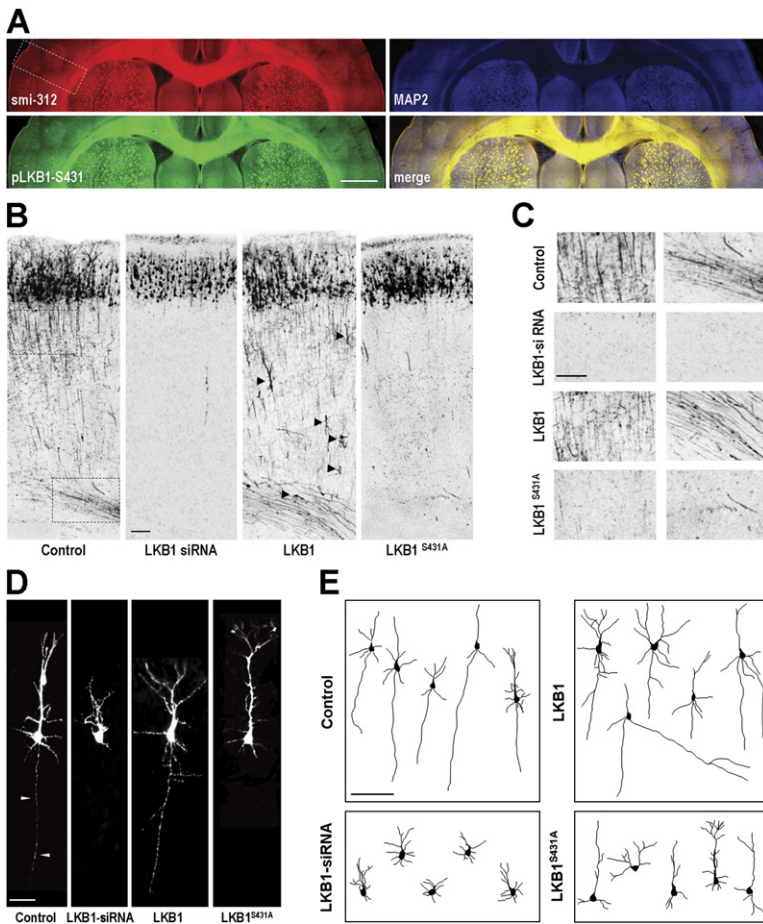


Figure 5. Downregulation of LKB1 or Overexpression of LKB1^{S431A} Abolished Axon Formation in Developing Cortical Neurons In Vivo

(A) Coronal sections of the somatosensory cortex of P7 rat brain, stained for smi-312 (red), pLKB1-S431 (green), and MAP2 (blue). Dotted lines indicate area for images in (B). Scale is 1 mm.

(B) Tomato fluorescence of P7 rat cortex transfected by in utero electroporation at E18 with Tomato together with various constructs as indicated. Scale is 100 μ m. Arrowheads indicate cells with apparent retarded migration.

(C) Higher magnification images (of boxed regions in B) showing radially oriented axons in cortical plate (left panels) and horizontally oriented axons near SVZ (right panels) for cortices transfected with various constructs.

(D) 2D projection of confocal images (in Tomato fluorescence) of typical cortical neurons in layer II/III of P7 cortex transfected with different constructs. Cells in regions of a low density of transfected cells were chosen for illustration. Scale is 25 μ m.

(E) Sample tracings of 2D projection of five cortical neurons transfected with different constructs as in (D). Scale is 100 μ m.

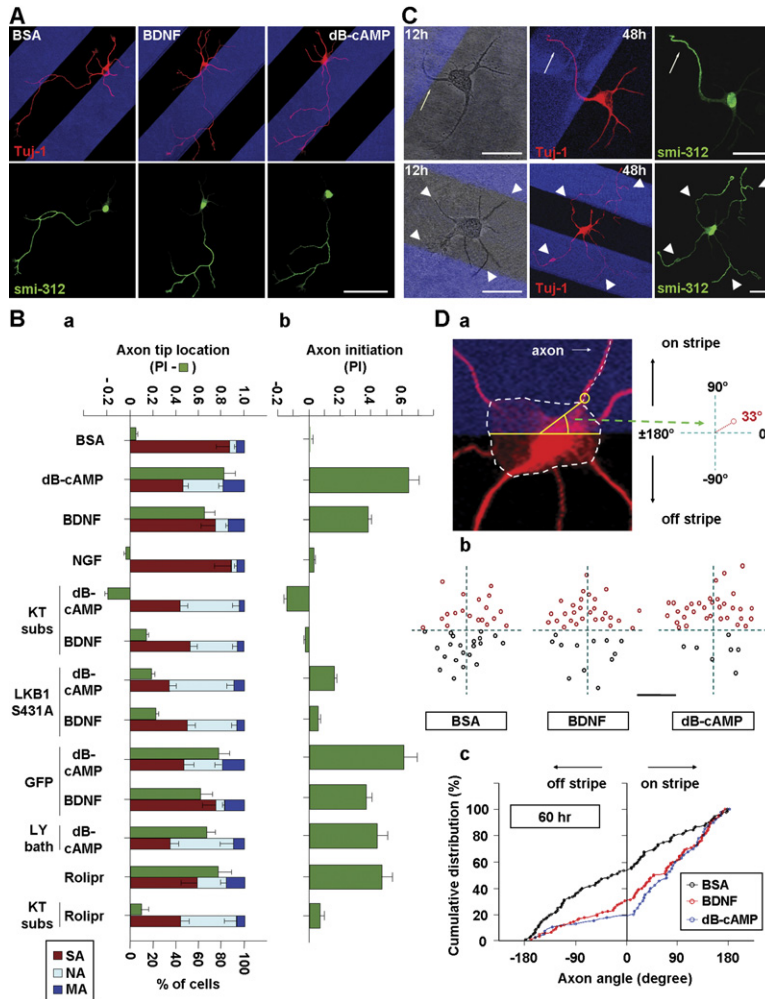
BDNF (Lohof et al., 1992; Song et al., 1997) or from an enhanced axon differentiation of neurites that were initiated on the stripe. The latter possibility was first suggested by the finding that neurites that encountered dB-cAMP (Figure 6C) or BDNF (data not shown) stripes at 12 hr were found to differentiate into axons by 48 hr. Furthermore, we analyzed the neurite initiation site on the soma for all polarized neurons whose soma was located at the stripe boundary (Figures 6A, 6Bb, and 6D). The angular distribution of the initiation site with respect to the stripe boundary was determined (Figure 6Da) for all neurites that became axons in 48–60 hr cultures. While neurites initiated “on” or “off” the BSA stripe showed equal frequency of becoming axons (PI = 0, Figure 6Bb), there was a much higher frequency for neurites initiated on dB-cAMP, BDNF, or rolipram stripes to become axons (Figure 6Bb). This was also shown by the distribution of the angle of axon initiation sites (Figures 6Db and 6Dc). Thus localized exposure of neurite to BDNF and dB-cAMP had indeed promoted axon initiation.

Analysis of the percentage of neurons exhibiting SA, NA, and MA phenotypes at 60 hr (Figure 6Ba) showed that cells plated on BSA- or NGF-stripped substrate had similar phenotypes as those on the control poly-L-lysine substrate, but those plated on BDNF or dB-cAMP striped

substrate exhibited reduced SA cells and increased NA and MA cells. This reduction of SA cells may be attributed to simultaneous contact of several neurites with the stripe that promoted differentiation of multiple axons (see Figures 6C and 6Ba). Furthermore, neurons with the soma located on BDNF, dB-cAMP, or rolipram stripes often exhibited no axons (Figure S7A), as was further confirmed by analyzing the phenotypes of cells with the soma on or off the stripes separately (Figure S9), suggesting that localized exposure of BDNF and local elevation of cAMP activity is important for the induction of axon differentiation.

Localized BDNF or dB-cAMP Exposure Induces pLKB1-S431 Accumulation

That LKB1 phosphorylation at S431 is important for axon differentiation (Figures 3E and S5C) is further supported by the finding that in 6–12 hr neurons pLKB1-S431 often accumulated only in the neurite that contacted the BDNF or dB-cAMP stripe (Figure 7A). For all neurons with the soma located at the stripe boundary, we found a clear preference for the pLKB1-S431-enriched neurite to be located on the BDNF or dB-cAMP stripe (Figure 7B), reminiscent of the preference of axon-initiation sites at the stripe boundary determined at 48–60 hr (Figure 6Dc).



60 hr. Each data point depicts one axon. Scale is 5 μ m. (c) Cumulative percentage plots for the axon-initiation angles for all cells. The data for BSA stripes ($n = 90$) were significantly different from those for BDNF ($n = 90$) or dB-cAMP ($n = 40$) stripes ($p < 0.001$, Kolmogorov-Smirnov test).

This resemblance supports the notion that localized exposure to BDNF and dB-cAMP triggers axon differentiation by inducing preferential accumulation of pLKB1-S431. Furthermore, the neurite in contact with the dB-cAMP stripe at 16 hr exhibited GFP-STRAD accumulation and differentiated into an axon by 48 hr (Figure 7C). When cells cultured on BDNF- or dB-cAMP-stripped substrates were examined at 60 hr, we found that pLKB1-S431 was predominantly expressed in the axon of SA (Figures 7Da–7Db) or MA cells (Figure 7Dc). Quantitative analysis showed strong correlation of pLKB1-S431 staining with smi-312 but not with MAP2 (data not shown). Moreover, for cells with their soma located on the dB-cAMP stripe, NA cells exhibited a low level of overall pLKB1-S431 immunostaining (Figures S7A and S7B), whereas SA cells showed high pLKB1-S431 staining in the axon. These results suggest that localized BDNF or cAMP signaling initiates axon differentiation through STRAD/LKB1 interaction and LKB1 phosphorylation.

Figure 6. Localized Exposure to BDNF or dB-cAMP Induces Axon Differentiation

(A) Hippocampal neurons in 60 hr cultures on substrates coated with BSA, BDNF, or dB-cAMP stripes (blue), immunostained for Tuj-1 and smi-312. Scale is 50 μ m.

(B) Preferential axon-tip location (a) and axon initiation (b) on substrates coated with BSA, dB-cAMP, BDNF, NGF, or rolipram stripes and stained for smi-312 and Tuj-1 at 3 DIV. Preference index (PI, defined in the text) was used to determine the axon-tip location (a) and preferential axon initiation (b) from all SA cells with soma located at the stripe boundary (see D). Percentages of cells showing NA, SA, or MA phenotypes (a; coded by color) are shown as average \pm SD ($n = 5$ cultures, 30–50 cells each). Treatments included transfection with GFP-LKB1^{S431A} or GFP. “KT subs”: cells were plated on substrate uniformly coated with KT5720 before stripe coating. “LY” indicates LY294002, bath-applied.

(C) Neurons on dB-cAMP striped substrate (blue), imaged at 12 and 48 hr, followed by staining for Tuj-1 and smi-312. Neurites encountering the stripe at 12 hr became axons at 48 hr for either SA (arrow) or MA cell (arrowheads). Scale is 25 μ m.

(D) Quantitation of stripe-induced preferential axon initiation. Axon initiation was examined for cells with soma located at the stripe boundary. (a) Schematic diagram depicts the angle of neurite initiation for neurites that became axons by 48 hr, either “on-stripe” (0° to 180°) or “off-stripe” (–180° to 0°). The angle was defined relative to the center of stripe boundary intersecting the soma (yellow line). (b) Angular distribution of axon-initiation sites for cells cultured on stripes of BSA, BDNF, or dB-cAMP (40 random sampled cells each), determined by smi-312 staining at

PKA Mediates Axon Differentiation Induced by BDNF or dB-cAMP

Bath application of PKA inhibitors KT5720 (0.2 to 1 μ M) or Rp-cAMPS (20 to 100 μ M) had no apparent effect on neuronal polarization on substratum uniformly coated with poly-lysine (Figure S8B), consistent with a previous report (Shi et al., 2003). However, when KT5720 or Rp-cAMPS was uniformly coated on the poly-lysine substrate, neuronal polarization was greatly impaired, with reduced SA cells and increased NA cells (Figures S8A and S8B), although the average total neurite length was not affected (Figure S8C; Substrate coating may have facilitated the cellular uptake of these poorly soluble drugs.). In contrast, inhibition of PI3K by bath application of LY294002 severely reduced both neuron polarization and total neurite length (Figures S8A–S8C). These results suggest that PKA activity is specifically required for spontaneous neuronal polarization but not for overall neurite growth. Further studies showed that preferential axon initiation

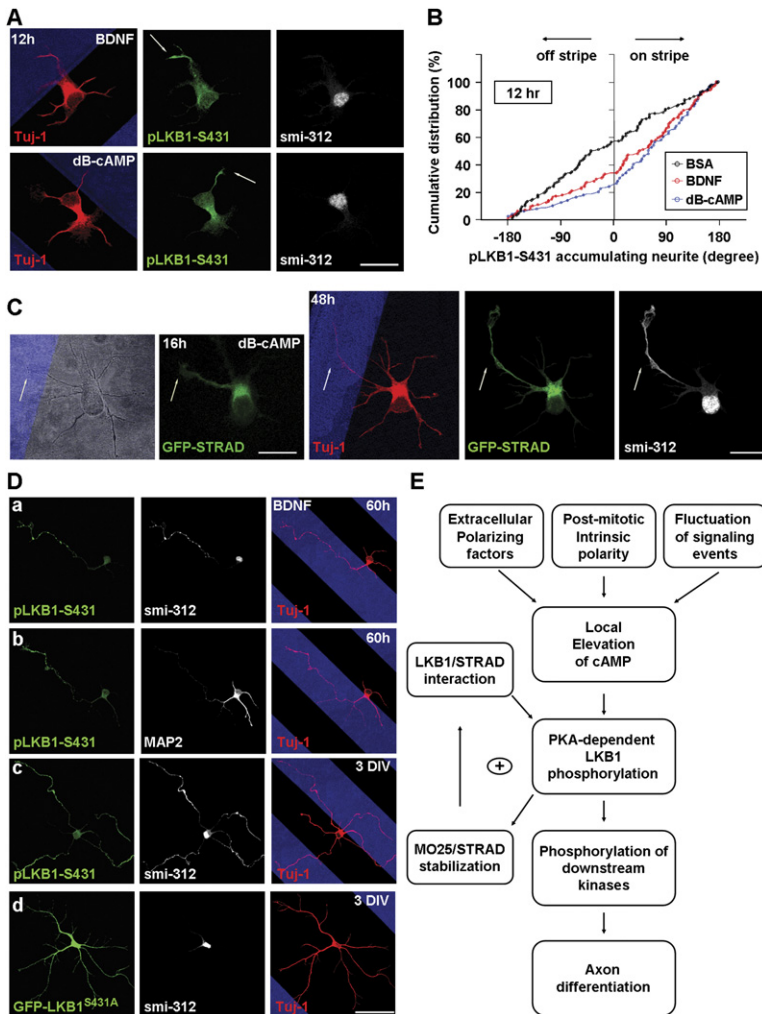


Figure 7. Axon Induction by BDNF and dB-cAMP Requires PKA-Dependent Phosphorylation of LKB1 at S431

(A) Neurons cultured for 12 hr on BDNF- or dB-cAMP-stripped substrate, coimmunostained with pLKB1-S431, Tuj-1, and smi-312, showing accumulation of pLKB1-S431 in the neurite (arrow) in contact with the stripe (blue). Scale is 25 μ m.

(B) Cumulative percentage plot of angular distribution of initiation sites for neurites showing pLKB1-431 accumulation at 12 hr on BSA, BDNF, or dB-cAMP stripes for all cells with soma located at stripe boundary. Data for BDNF (n = 100) or dB-cAMP (n = 50) were significantly different from those for BSA (n = 100; p < 0.001, Kolmogorov-Smirnov test).

(C) Neuron cultured on dB-cAMP-stripped substrate and transfected with GFP-STRAD, imaged at 16 hr, and stained for smi-312 and Tuj-1 at 48 hr. Neurite contacting the stripe at 16 hr exhibited GFP-STRAD accumulation and became an axon by 48 hr. Scale is 25 μ m.

(D) Neurons cultured on BDNF-stripped substrate for 3 days. (a and b) An SA cell with axon differentiation on the BDNF stripe, stained for pLKB1-S431 together with Tuj-1 and smi-312 (a) or MAP2 (b). (c) A MA cell similarly stained as in (a). (d) An NA cell transfected with GFP-LKB1^{S431A} and stained with Tuj-1 and smi-312. Scale is 50 μ m.

(E) A positive feedback model for axon initiation: (1) The presence of extracellular polarization factors, the asymmetry in the distribution of cytoplasmic factors after mitotic division, or stochastic fluctuation of signaling events may all trigger an initial elevation of cAMP level in one undifferentiated neurite, leading to localized PKA-dependent LKB1 phosphorylation. (2) Localized LKB1 phosphorylation and PKA-dependent MO25 stabilization facilitate the

local formation of LKB1/STRAD/MO25 heterotrimeric complex, which promotes LKB1/STRAD interaction, leading to a further increase in the local level of phosphorylated LKB1. (3) PKA-dependent LKB1 phosphorylation activates its kinase activity, resulting in phosphorylation of downstream effectors responsible for axon initiation.

induced by BDNF or dB-cAMP stripes was mediated through PKA because this effect was greatly diminished when cells were plated on BDNF, dB-cAMPs, or rolipram-stripped substrate that was uniformly precoated with KT5720 (Figure 6Bb). Interestingly, bath application of LY294002 did not affect preferential axon initiation of SA cells induced by the dB-cAMP stripes (Figure 6Bb), suggesting that PI3K and cAMP signaling may represent parallel pathways that contribute to axon differentiation.

Critical Role of pLKB1-S431 in BDNF- and cAMP-Induced Axon Differentiation

When cultures plated on the BDNF- or dB-cAMP-stripped substrate were transfected with GFP-LKB1^{S431A} and examined at 60 hr, we found a clear increase in the NA population (Figure 6Ba). These transfected cells failed to initiate axons on BDNF stripes despite extensive neurite growth (Figure 7Dd), as compared to untransfected cells

(Figures 7Da–7Dc). Moreover, the SA population of these transfected cells showed a greatly reduced preferential axon-tip location and preferential axon initiation at the stripe boundary (Figure 6B). A subpopulation of GFP-LKB1^{S431A}-transfected cells exhibited normal polarization with single axon (SA), possibly because they had lower levels of GFP-LKB1^{S431A} expression, as suggested by the finding that these SA cells exhibited significantly lower GFP-LKB1^{S431A} expression than NA cells (Figure S8D). Analysis of the total pLKB1-S431 immunostaining in cells plated on striped substrates under all conditions further showed that pLKB1-S431 level is significantly higher in SA cells than NA cells for cells plated on control BSA stripes or BDNF stripes and that BDNF-stripped substrate had increased the pLKB1-S431 level in SA cells, and this increase was abolished by KT5720 (Figure S8E). Together, these findings support the notion that PKA-dependent phosphorylation of LKB1 at S431 promotes axon initiation.

DISCUSSION

Early Events in Axon Initiation

How an axon emerges from several initially morphologically equivalent neurites is an outstanding question. The finding that the plus-end motor protein KIF5C selectively translocates among different undifferentiated neurites until it is localized to the future axon (Jacobson et al., 2006) suggests an early, modifiable fate of the neurite. Candidates for the early determinant of axon differentiation, e.g., plasma membrane ganglioside sialidase (PMGS; Da Silva et al., 2005) and the brain-specific protein shootin1 (Toriyama et al., 2006), are localized at the growing tip of undifferentiated neurite. However, we found that LKB1/STRAD is accumulated over the entire undifferentiated neurite. The tip localization of PMGS suggests a more direct association with the initiation of accelerated neurite growth, whereas LKB1/STRAD accumulation over the neurite may reflect a global asymmetry created within the neuron that facilitates the actions of other factors in axon differentiation. On a uniform substrate, the early asymmetry of LKB1/STRAD distribution may result from either a predetermined somatic asymmetry or a stochastic process. However, localized exposure to the extracellular BDNF and dB-cAMP can bias the LKB1/STRAD accumulation and activation, leading to preferential axon initiation. Downregulation of LKB1, overexpression of LKB1^{S431A}, or treatment with PKA inhibitors all resulted in the failure of axon differentiation without a significant effect on the overall neurite growth, suggesting that LKB1 does not affect the overall growth capacity of the neuron (Figures 3D, 3E, S8A, and S8C). However, local LKB1/STRAD accumulation may act by biasing the growth capacity toward one neurite, and localized BDNF or dB-cAMP may promote axon initiation by biasing neurite growth through LKB1 accumulation and activation.

Positive Feedback Mechanism for LKB1 Localization and Phosphorylation

During epithelia polarization, STRAD is an essential cofactor for LKB1 function (Baas et al., 2004), coordinating both the cytoplasmic localization of LKB1 and activation of its catalytic activity (Boudeau et al., 2003). Our heterologous expression studies showed that complex formation between coexpressed LKB1 and STRAD indeed increases LKB1 phosphorylation and results in mutual protein stabilization (Figure 1). Interestingly, LKB1/STRAD-complex formation is promoted by the coexpression of a scaffolding protein MO25 (Boudeau et al., 2003; Figure 4), and downregulation of MO25 dramatically reduced the level of LKB1 protein (Boudeau et al., 2003). Conversely, LKB1 also facilitates MO25/STRAD interaction since coexpression with LKB1 and the binding of LKB1 to STRAD generate additional binding sites for MO25 within the LKB1-STRAD complex (Boudeau et al., 2003). We further showed that cAMP elevation increases the MO25 protein level (Figure 4), probably through the interaction with endogenous STRAD. The association of LKB1 with STRAD results in

the phosphorylation of LKB1 at several sites, including the evolutionarily conserved PKA site S431 (Martin and St Johnston, 2003). We found that LKB1 phosphorylation at S431 is critical for axon initiation since overexpressing LKB1^{S431A} inhibited axon formation both in vitro and in vivo, presumably by interfering with the association of STRAD or other proteins important for LKB1 function, thus hindering endogenous LKB1 stabilization and phosphorylation. Taken together, our results support the model (Figure 7E) that local cAMP elevation results in local accumulation of LKB1/STRAD/MO25 heterotrimeric complex, leading to enhanced LKB1/STRAD interaction and a further increase in local LKB1 phosphorylation and activation. This positive feedback helps to establish a stable LKB1 activity in the neurite that further activates downstream effectors for axon initiation.

Downstream Effectors of Activated LKB1

Phosphorylation of GSK-3 β by PI3K and the consequent inactivation of this constitutively active kinase at the growth cone are important for axon differentiation (Yoshimura et al., 2005; Jiang et al., 2005). In developing *Xenopus* embryo, the LKB1 ortholog XEEK1 directly associates with aPKC and modulates aPKC-mediated phosphorylation of GSK-3 β on Ser-9 (Ossipova et al., 2003). Thus, LKB1 may lie upstream to GSK-3 β and local cAMP elevation in the undifferentiated neurite may induce PKA-dependent phosphorylation of GSK-3 β on Ser-9, and BDNF-induced phosphorylation of GSK-3 β may also depend on the cAMP pathway in addition to the PI3K pathway. In addition, the family of AMP-activated protein kinases (AMPKs), including the microtubule affinity-regulating kinase (MARK)/PAR-1, lies downstream of LKB1 (Lizcano et al., 2004). Recent studies using genetic deletion in mice have demonstrated the direct involvement of PAR-1-related kinases, the mammalian SAD-A and SAD-B (BRSK1/2), in neuronal polarization by local regulation of phosphorylation of the axonal microtubule-binding protein Tau (Kishi et al., 2005). By selective deletion of the LKB1 gene in the forebrain, Barnes et al. (2007) show in this issue of *Cell* that LKB1 is required for axon formation in the embryonic cortex in vivo and that axon-specific phosphorylation of LKB1 is required for its function in axon formation. Since SAD is expressed in both axons and dendrites of polarized neurons (Kishi et al., 2005), preferential localization and activation of LKB1 to the undifferentiated neurite may initiate axon development via SAD phosphorylation and its downstream actions.

Upstream Signaling for LKB1 Activation

We found that cAMP signaling locally is sufficient to induce axon differentiation, and this effect is mediated at least in part through PKA-dependent LKB1 phosphorylation at S431. Interestingly, substrate-coated PKA inhibitor greatly reduced spontaneous neuronal polarization without affecting the overall neurite growth, whereas the PI3K inhibitor affected both polarization and overall growth (Figures S8A–S8C). Since PKA inhibitors abolished

the biased axon initiation on the dB-cAMP stripe whereas the PI3K inhibitor had no effect (Figure 6B), cAMP signaling may act either in parallel or on downstream effectors of the PI3K pathway in promoting axon initiation. Finally, in line with recent findings that axon guidance cues UNC-6/Netrin and Wnt serve a function in neuronal polarization by initiating axon formation in *C. elegans* (Adler et al., 2006; Hilliard and Bargmann, 2006), we found that the BDNF can induce both chemotropic growth-cone turning and axon initiation in cultured hippocampal neurons. Whether BDNF and other extracellular factors that elevate cAMP signaling indeed serve as neuron polarization factors in vivo remains to be examined.

EXPERIMENTAL PROCEDURES

Cell Cultures, Transfection, Immunoblotting, and Immunostaining

Cultures of dissociated hippocampal neurons were prepared from embryonic E18 rats as previously described (Dotti et al., 1988) and were cultured in neurobasal medium (Invitrogen) supplemented with B-27 (Invitrogen). Transfections were carried out 4 hr after plating using Lipofectamine 2000 (Invitrogen). HEK293T cells were grown in DMEM medium supplemented with 10% FBS and were transiently transfected using the calcium-phosphate method. For analysis of LKB1 phosphorylation by immunoblotting, cells were treated with forskolin (20 μ M) or dB-cAMP (20 μ M) for 45 min; with BDNF (50 ng/ml) for 15 min, either alone or in combination with inhibitors (KT5720, 200 nM; Rp-cAMP, 20 μ M; rolipram, 0.5 μ M; and LY294002, 20 μ M), which were added 2 hr prior to stimulation with the agonist. Cell extracts were prepared at 4 DIV for neurons and two days after transfection for HEK293T cells. For immunostaining, cultured neurons were fixed with 4% formaldehyde in PBS for 10 min, followed by 10 min treatment with 0.1% Triton X-100 and 2 hr blocking with 10% NGS. For in vivo studies, brains were fixed by transcardial perfusion of 4% paraformaldehyde and sectioned coronally at the level of the somatosensory cortex, and 80 μ m slices were immunostained as the procedure for cultured neurons.

Phenotype Classification and Quantitation of Fluorescence

Neurons were categorized into three phenotypes: single axon (SA), multiple axons (MA), and no axon (NA). In most cases the axon was defined by axon-specific immunostaining of smi-312. Neurite length was also used in some cases for assessing axon differentiation by the following criteria (which were confirmed by smi-312 staining): a process more than 2.5 times longer than other processes and longer than 230 μ m (4 DIV) or 120 μ m (60 hr) was considered an axon. Imaging was performed using a confocal laser microscope (Leica DM IRBE) with a 40 \times oil-immersion objective (NA 1.28). For immunostained slices, images (average of three acquisitions for each focal plane) were acquired with a 10 \times dry objective (NA 0.3). For morphometric analysis, images of cells with Tomato fluorescence colocalizing with EGFP fluorescence were acquired. Confocal images (50–70 μ m Z stacks) of isolated cells were acquired, and 2D projections were used for tracing neurite arbors. The image acquisition and data analysis were performed in a blind manner.

Statistical Analysis

To decide the statistical test for the comparison between two data sets, we first examined whether the data in each set are normally distributed (Jarque-Bera test). If both data sets showed normal distribution, we used the parametric test (t test); otherwise, we used the non-parametric test (Kolmogorov-Smirnov test). For comparison involving multiple data sets, we performed nonparametric ANOVA (Friedman's

test) to examine whether at least one data set is different from the rest and then further examined the difference between two individual data sets using t test or Kolmogorov-Smirnov test, depending on whether the data are normally distributed. Bootstrap analysis was used to determine the probability for the coincidence of two events to occur by chance (see Supplemental Experimental Procedures).

Procedures for preparing plasmid constructs, generation of siRNAs, in utero electroporation, microfabrication and substrate patterning, and sources of antibodies and chemicals are provided in Supplemental Experimental Procedures.

Supplemental Data

Supplemental Data include Experimental Procedures and nine figures and can be found with this article online at <http://www.cell.com/cgi/content/full/129/3/565/DC1/>.

ACKNOWLEDGMENTS

We thank R. Thaker, S. Li, M. Nasir, and D. Liepmann for help with PDMS microfluidic molds; H.F. Gao for the help with culture preparations; and X.B. Yuan for providing the various constructs. This work was supported by a grant from NIH (NS-22764).

Received: October 28, 2006

Revised: February 26, 2007

Accepted: April 9, 2007

Published: May 3, 2007

REFERENCES

- Adler, C.E., Fetter, R.D., and Bargmann, C.I. (2006). UNC-6/Netrin induces neuronal asymmetry and defines the site of axon formation. *Nat. Neurosci.* 9, 511–518.
- Alessi, D.R., Sakamoto, K., and Bayascas, J.R. (2006). LKB1-dependent signaling pathways. *Annu. Rev. Biochem.* 75, 137–163.
- Arimura, N., and Kaibuchi, K. (2007). Neuronal polarity: from extracellular signals to intracellular mechanisms. *Nat. Rev. Neurosci.* 8, 194–205.
- Baas, A.F., Boudeau, J., Sapkota, G.P., Smit, L., Medema, R., Morrice, N.A., Alessi, D.R., and Clevers, H.C. (2003). Activation of the tumor suppressor kinase LKB1 by the STE20-like pseudokinase STRAD. *EMBO J.* 22, 3062–3072.
- Baas, A.F., Kuipers, J., van der Wel, N.N., Battle, E., Koerten, H.K., Peters, P.J., and Clevers, H.C. (2004). Complete polarization of single intestinal epithelial cells upon activation of LKB1 by STRAD. *Cell* 116, 457–466.
- Barnes, A.P., Lilley, B.N., Pan, Y.A., Plummer, L.J., Powell, A.W., Raines, A.N., Sanes, J.R., and Polleux, F. (2007). LKB1 and SAD kinases define a pathway required for the polarization of cortical neurons. *Cell* 129, this issue, 549–563.
- Boudeau, J., Baas, A.F., Deak, M., Morrice, N.A., Kieloch, A., Schutkowski, M., Prescott, A.R., Clevers, H.C., and Alessi, D.R. (2003). MO25 α/β interact with STRAD α/β enhancing their ability to bind, activate and localize LKB1 in the cytoplasm. *EMBO J.* 22, 5102–5114.
- Chen, Y.M., Wang, Q.J., Hu, H.S., Yu, P.C., Zhu, J., Drewes, G., Pivnicka-Worms, H., and Luo, Z.G. (2006). Microtubule affinity-regulating kinase 2 functions downstream of the PAR-3/PAR-6/atypical PKC complex in regulating hippocampal neuronal polarity. *Proc. Natl. Acad. Sci. USA* 103, 8534–8539.
- Craig, A.M., and Banker, G. (1994). Neuronal polarity. *Annu. Rev. Neurosci.* 17, 267–310.
- Da Silva, J.S., Hasegawa, T., Miyagi, T., Dotti, C.G., and Abad-Rodriguez, J. (2005). Asymmetric membrane ganglioside sialidase activity specifies axonal fate. *Nat. Neurosci.* 8, 606–615.

- de Anda, F.C., Pollarolo, G., Da Silva, J.S., Camoletto, P.G., Feiguin, F., and Dotti, C.G. (2005). Centrosome localization determines neuronal polarity. *Nature* 436, 704–708.
- Dotti, C.G., Sullivan, C.A., and Banker, G.A. (1988). The establishment of polarity by hippocampal neurons in culture. *J. Neurosci.* 8, 1454–1468.
- Gao, Y., Nikulina, E., Mellado, W., and Filbin, M.T. (2003). Neurotrophins elevate cAMP to reach a threshold required to overcome inhibition by MAG through extracellular signal-regulated kinase-dependent inhibition of phosphodiesterase. *J. Neurosci.* 23, 11770–11777.
- Hilliard, M.A., and Bargmann, C.I. (2006). Wnt signals and frizzled activity orient anterior-posterior axon outgrowth in *C. elegans*. *Dev. Cell* 10, 379–390.
- Inagaki, N., Chihara, K., Arimura, N., Menager, C., Kawano, Y., Matsuo, N., Nishimura, T., Amano, M., and Kaibuchi, K. (2001). CRMP-2 induces axons in cultured hippocampal neurons. *Nat. Neurosci.* 4, 781–782.
- Jacobson, C., Schnapp, B., and Banker, G.A. (2006). A change in the selective translocation of the Kinesin-1 motor domain marks the initial specification of the axon. *Neuron* 49, 797–804.
- Jiang, H., Guo, W., Liang, X., and Rao, Y. (2005). Both the establishment and the maintenance of neuronal polarity require active mechanisms: critical roles of GSK-3 β and its upstream regulators. *Cell* 120, 123–135.
- Kishi, M., Pan, Y.A., Crump, J.G., and Sanes, J.R. (2005). Mammalian SAD kinases are required for neuronal polarization. *Science* 307, 929–932.
- Lizcano, J.M., Goransson, O., Toth, R., Deak, M., Morrice, N.A., Boudeau, J., Hawley, S.A., Udd, L., Makela, T.P., Hardie, D.G., and Alessi, D.R. (2004). LKB1 is a master kinase that activates 13 kinases of the AMPK subfamily, including MARK/PAR-1. *EMBO J.* 23, 833–843.
- Lohof, A.M., Quillan, M., Dan, Y., and Poo, M.M. (1992). Asymmetric modulation of cytosolic cAMP activity induces growth cone turning. *J. Neurosci.* 12, 1253–1261.
- Martin, S.G., and St Johnston, D.S. (2003). A role for *Drosophila* LKB1 in anterior-posterior axis formation and epithelial polarity. *Nature* 421, 379–384.
- Nishimura, T., Kato, K., Yamaguchi, T., Fukata, Y., Ohno, S., and Kaibuchi, K. (2004). Role of the PAR-3-KIF3 complex in the establishment of neuronal polarity. *Nat. Cell Biol.* 6, 328–334.
- Ossipova, O., Bardeesy, N., DePinho, R.A., and Green, J.B.A. (2003). LKB1 (XEEK1) regulates Wnt signaling in vertebrate development. *Nat. Cell Biol.* 5, 889–894.
- Pearse, D.D., Periera, F.C., Marcillo, A.E., Bates, M.L., Berrocal, Y.A., Filbin, M.T., and Bunge, M.B. (2004). cAMP and Schwann cells promote axonal growth and functional recovery after spinal cord injury. *Nat. Med.* 10, 610–616.
- Saito, T., and Nakatsuji, N. (2001). Efficient gene transfer into the embryonic mouse brain using in vivo electroporation. *Dev. Biol.* 240, 237–246.
- Sapkota, G.P., Kieloch, A., Lizcana, J.M., Lain, S., Arthur, J.S.C., Williams, M.R., Morrice, N., Deak, M., and Alessi, D.R. (2001). Phosphorylation of the protein kinase mutated in Peutz-Jeghers cancer syndrome, LKB1/STK11 at Ser⁴³¹ by p90^{RSK} and cAMP-dependent protein kinase, but not its farnesylation at Cys⁴³³, is essential for LKB1 to suppress cell growth. *J. Biol. Chem.* 276, 19469–19482.
- Schwamborn, J.C., and Puschel, A.W. (2004). The sequential activity of the GTPases Rap1B and Cdc42 determines neuronal polarity. *Nat. Neurosci.* 7, 923–929.
- Shi, S.H., Jan, L.Y., and Jan, Y.N. (2003). Hippocampal neuronal polarity specified by spatially localized mPar3/mPar6 and PI 3-kinase activity. *Cell* 112, 63–75.
- Song, H.J., Ming, G.L., and Poo, M.M. (1997). cAMP-induced switching in turning direction of nerve growth cones. *Nature* 388, 275–279.
- Sosa, L., Dupraz, S., Laurino, L., Bollati, F., Bisbal, M., Caceres, A., Pfenninger, K.H., and Quiroga, S. (2006). IGF-1 receptor is essential for the establishment of hippocampal neuronal polarity. *Nat. Neurosci.* 9, 993–995.
- Sternberger, L.A., Harwell, L.W., and Sternberger, N.H. (1982). Neurotypy: regional individuality in rat brain detected by immunocytochemistry with monoclonal antibodies. *Proc. Natl. Acad. Sci. USA* 79, 1326–1330.
- Toriyama, M., Shimada, T., Kim, K.B., Mitsuba, M., Nomura, E., Katsuta, K., Sakumura, Y., Roepstorff, P., and Inagaki, N. (2006). Shootin1: a protein involved in the organization of an asymmetric signal for neuronal polarization. *J. Cell Biol.* 175, 147–157.
- Wodarz, A. (2002). Establishing cell polarity in development. *Nat. Cell Biol.* 4, E39–E44.
- Yoshimura, T., Kawano, Y., Arimura, N., Kawabata, S., Kikuchi, A., and Kaibuchi, K. (2005). GSK-3 regulates phosphorylation of CRMP-2 and neuronal polarity. *Cell* 120, 137–149.